



## **Comparative seismic risk assessment of the residential buildings for a strong earthquake scenario in Iceland using local vs. global models**

**Darzi Atefe** – Faculty of Civil and Environmental Engineering, University of Iceland, Reykjavik, Iceland, e-mail: atefe@hi.is

**Bessason Bjarni** – Faculty of Civil and Environmental Engineering, University of Iceland, Reykjavik, Iceland, e-mail: bb@hi.is

**Halldorsson Benedikt** – Faculty of Civil and Environmental Engineering, University of Iceland, Reykjavik, Iceland, e-mail: skykkur@hi.is, Division of Processing and Research, Icelandic Meteorological Office, Reykjavik, Iceland, e-mail: benedikt@vedur.is

**Moosapoor Mojtaba** – Faculty of Civil and Environmental Engineering, University of Iceland, Reykjavik, Iceland, e-mail: mom12@hi.is

**Abstract:** Iceland is the most seismically active region in northern Europe and damaging earthquakes repeatedly occur in the South Iceland Seismic Zone (SISZ), a relatively densely populated region accommodating all critical infrastructures and lifelines. The most recent damaging earthquake in the SISZ was the  $M_w$ 6.3, 29-May-2008 Ölfus earthquake that occurred in close vicinity of the Hveragerði town. The town experienced intense near-fault strong-motion recorded on a strong-motion array (ICEARRAY I). To understand the consequences that a strong earthquake can cause in a high seismic region in terms of damage probability and damage-to-cost ratio, and to identify the most vulnerable building typologies, we perform seismic risk analyses for the Ölfus earthquake scenario across Hveragerði. Having detailed ground-motion data and a complete building exposure database give the unique opportunity to perform loss estimation in a high geographical resolution of building-by-building, contrary to the common municipality-based resolution. To this end, we employed the Empirical Bayesian Kriging method to estimate the intensity measures at building locations as well as account for the impact of their variability on the expected seismic loss. Finally, the risk metrics resultant from the global fragility curves developed as part of the global seismic risk model are compared with the most recent local models.

**Keywords:** Scenario-based loss estimation, building exposure, intensity measure, Empirical Bayesian Kriging, Iceland, Ölfus earthquake

### **1. Introduction**

Iceland is the most seismically active country in northern Europe. Over the last millennium, repeated strong ground shaking has occurred in the South Iceland Seismic Zone (SISZ), one of the two major transform zones of the country. The SISZ is a sinistral transform zone consisting of an array of parallel N-S striking dextral strike-slip faults, where earthquakes up to  $M_w$ 7.0 have occurred in its easternmost part. The SISZ is a predominantly flat rural agricultural region with a few relatively populated towns and all critical infrastructure and lifelines of modern-day society. Fig. 1 illustrates the epicenters of instrumentally recorded earthquakes by international agencies in SW Iceland (Jónsson et al. 2021). Fig. 1 also shows recording stations of the Icelandic Seismic Network (SIL), Icelandic strong motion network (ISMN), and the small-aperture strong-motion array (ICEARRAY I) located in Hveragerði. Hveragerði (red polygon in Fig. 1) is one of the small, populated towns located in the Ölfus region in the SISZ and one of the country's

tourist destinations with many critical infrastructure facilities. The town is the main subject of this study. Through the centuries, the Ölfus region has been hit by several destructive earthquakes. The most recent destructive earthquake striking the town was the 29 May 2008 Ölfus earthquake with  $M_w$ 6.3 (yellow star in Fig. 1). Despite the Ölfus earthquake being the costliest natural disaster in Iceland to date and causing widespread damage, there were however no collapsed residential buildings and no casualties.

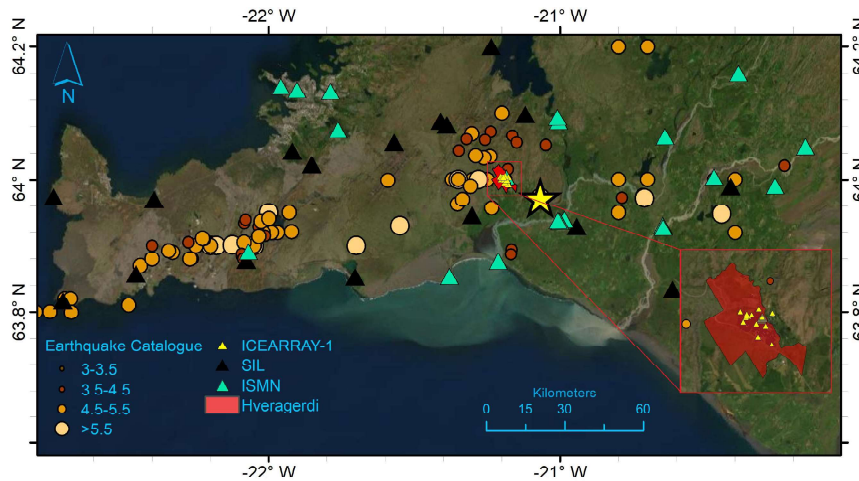


Fig. 1 - A map of SW-Iceland showing earthquake occurrences from 1904-2019 (Jónasson et al. 2021). The May 2008 Ölfus earthquake is displayed by a yellow star. In the middle of the SISZ (red box), the ICEARRAY I stations are depicted by yellow triangles over the Hveragerði town (red polygon).

To the best of the authors knowledge, there are only a few studies on seismic loss estimation risk assessment for Iceland. Rupakhety et al. (2016) simulated damage for a macroseismic hazard scenario corresponding to the Ölfus earthquake using ATC-13 (1985) vulnerability models and buildings vulnerability defined in terms of damage probability matrices derived from June 2000 earthquake damage data (Sigbjörnsson et al. 2007). They stated that ATC-13 vulnerability models should be used with caution in Iceland because although they seem suitable for Icelandic buildings undergoing small levels of damage, their efficacy for larger damage levels is not guaranteed. Besides, they indicated that creating vulnerability models based on MMI becomes problematic.

The Natural Catastrophe Insurance of Iceland (NCI, 2021) owns a fully probabilistic bespoke model for Icelandic earthquake risk assessment and a quick response deterministic model that can model scenarios such as major historical earthquakes to compute the insurance risk routinely based on 19 building classes (Bjarnason et al. 2016). However, the models, detail of the required assumptions and information as well as the corresponding results are not shared publicly. Using an open flexible risk assessment tool, like SELINA (Molina et al. 2010) through which any modification can be easily implemented, and the results can be regenerated by users is of great benefit for seismic risk modelers.

In Iceland, all properties, including residential dwellings, are registered in a detailed official database (Registers Iceland, 2020). This allows us to construct a detailed building exposure data of Hveragerði, thereby, enabling scenario-based seismic risk assessment on a high geographical resolution compared to the common risk analyses in the prevalent municipality level, which is based on the aggregated exposure data.

One of the main objectives of this study is to perform earthquake loss prediction in building-by-building spatial resolution for a scenario event corresponding to the damaging 2008 Ölfus earthquake across Hveragerði town. To estimate the ground motion intensity

measures (IMs) required for risk analyses in building-by-building spatial resolution level while accounting for their incorporated uncertainty, we employed an advance geostatistical procedure, the Empirical Bayesian Kriging (EBK) method, incorporating the high-quality acceleration time histories of the Ölfus earthquake recorded by the dense urban ICEARRAY I stations. The kriging geostatistical method is a widespread technique used for spatial interpolation, considering spatial variability. Kriging uses the variogram model to compute localized weighting parameters, in essence, the weights of neighboring points based on the distribution of those values. In Costanzo (2018), two geostatistical techniques of the Kriging method and co-kriging have been benchmarked and tested on earthquakes of 2016-2017 central Italy to derive shake maps for cumulative absolute velocity and Arias intensity parameters. Finally, we predict different risk metrics employing both local and global fragility and vulnerability models developed recently and compare their performance for the building typologies identified based on the SERA taxonomy scheme.

## 2. The residential building exposure database

A complete building property database ([www.skra.is](http://www.skra.is)), including key information for each building, e.g., construction year, building material, number of storeys, floor area, replacement value, etc., are provided for residential buildings in Hveragerði town constructed before the May 2008 Ölfus earthquake and then, linked to the Open Street Map building polygons for clear spatial visualization. Fig. 2 indicates the number of buildings in Hveragerði grouped by construction material and year of construction. The database comprised 55.6% reinforced concrete including concrete and precast concrete classes (RC), 38% timber (W), and 6.4% unreinforced masonry buildings including cinderblock, bricks and concrete combination with blocks/bricks (MUR) (Fig. 2a). Table 1 shows the lateral force coefficient for RC buildings located in the zones with the highest seismic hazard in Iceland defined by different seismic design codes that were in practice in Iceland, see also Crowley et al. (2021). Moreover, the code classification of buildings ranging from no-code (CDN) to high-code (CDH) as well as the percentage of buildings in each class (also in Fig. 2b) are presented in Table 1.

The first seismic code (ÍST 13) was then implemented in Iceland in 1976. Therefore, concrete buildings constructed before had a limited amount of reinforcement, typically only around the openings in structural walls (low code, CDL in Table 1). In total, ~46.2% of buildings were constructed before the first seismic code (CDN+CDL). Generally, the Icelandic building stock is considered young in an international context since no existing building was built before 1870 (Bessason et al. 2020). In 1989, the seismic code was upgraded and put into practice until 2002. The 1976-2002 period features the moderate code period (CDM) in Iceland as almost similar lateral force coefficients were in use for seismic design. CDM class includes 31.2% of buildings in Hveragerði.

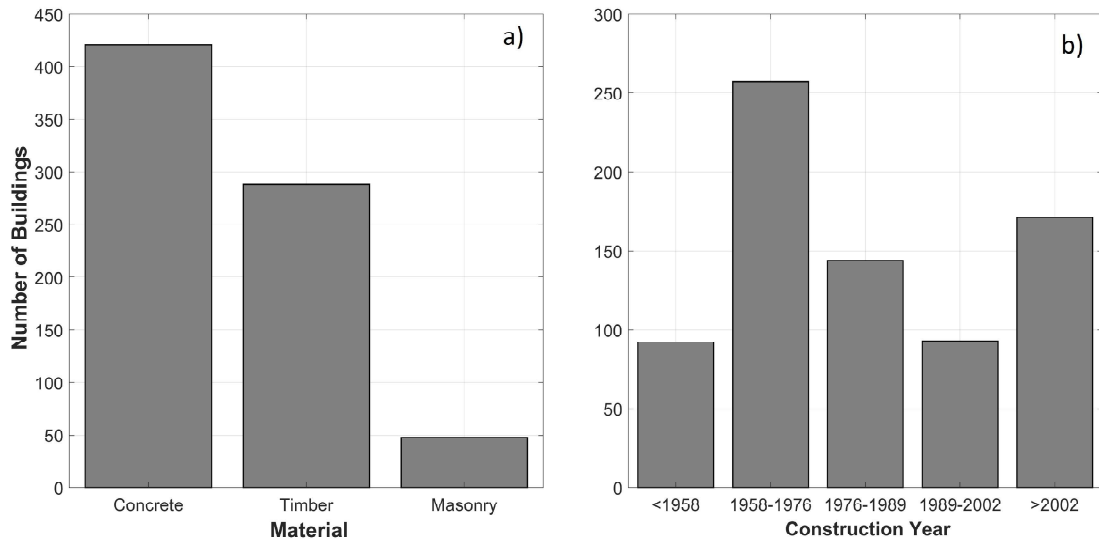


Fig. 2 - a) Histogram of a number of buildings against (a) construction material and (b) year of construction.

In 2002, when Eurocode 8 and the National Application Documents were implemented in Iceland (SI 2002), the lateral force coefficient defined by the design spectrum increased incredibly from 0.16g to 0.33g, thus presenting the high-code period (CDH). Here, a behavior factor corresponding to the medium ductility class is assumed. The same conclusion was drawn for the European building stock after the implementation of Eurocode 8 (Crowley et al. 2021).

In Iceland, structural walls dominate the lateral load resisting system (LLRS) in almost all buildings, regardless of the construction material or typologies. This contradicts other regions such as southern Europe, where moment-frames with or without masonry/brick infills are commonly used for constructing residential buildings. Moreover, almost all buildings are low-rise with less than two storeys (97.7%).

Table 1: Lateral force coefficient and percentage of buildings corresponding to seismic design codes

| Period      | Lateral Force Coefficient | Seismic Design Code                                     | Code Classification | Buildings % |
|-------------|---------------------------|---|---------------------|-------------|
| < 1958      | -                         | No code   | CDN                 | 12.2%       |
| 1958 - 1976 | 0.07-0.1                  | Only hazard map (Tryggvason et al. 1958)                | CDL                 | 34%         |
| 1976 - 1989 | 0.133                     | Seismic code ÍST 13 (Iðnþróunarstofnun Íslands, 1976)   | CDM                 | 19.7%       |
| 1989 - 2002 | 0.16                      | seismic code ÍST 13 (Iðntæknistofnun Íslands, 1989)     |                     | 11.5%       |
| 2002 - 2010 | 0.33                      | Eurocode 8 and National Application Documents (SI 2002) | CDH                 | 22.6%       |
| > 2010      | 0.42                      | Eurocode 8 and Icelandic National Annexes (SI 2010)     |                     | 0           |

### 3. Shake maps of ground motion intensity measures

In this study, the PGA and pseudo acceleration response spectrum (PSA) at 0.3 sec are used as the IMs representing the fundamental period of structures in Hveragerði for which the fragility curves are available. The IMs are calculated from the time histories of the Ölfus earthquake recorded by ICEARRAY I stations. In this study, the horizontal components of ground motion measures are combined to the average rotation-invariant

(ARI) measure which gives the expected values of PSA for all possible orientation of accelerometer axes in the horizontal plane (Rupakhety and Sigbjörnsson 2013).

To model the likely ground motions at non-recording sites we use geostatistical interpolation methods to estimate the values in unsampled locations and thus project the observed data into a continuous form in raster data format. To this end, we carry out EBK geostatistical analyses to generate shake maps (spatial interpolation) (left panels of Fig. 3) and their corresponding uncertainty maps for the selected IMs (right panels of Fig. 3). Compared to the classical Kriging method, EBK employs hundreds of semivariogram models that have significant benefits such as more accurate prediction, in particular for small datasets, more accurate standard errors of prediction, and minimal interactive modelling (Krivoruchko and Gribov 2019). Following that we extract the estimated IMs at building locations (grey polygons in Fig. 3) along with its variation to allow carrying out seismic risk analyses at building-by-building geographical resolution. As per our expectation, the spatial areas with low standard errors remarked around ICEARRAY I sites indicates indicate our full confidence in the estimated IMs. But, as the distance from the observation sites increases, the uncertainty increases as well, e.g., outside of the array area.

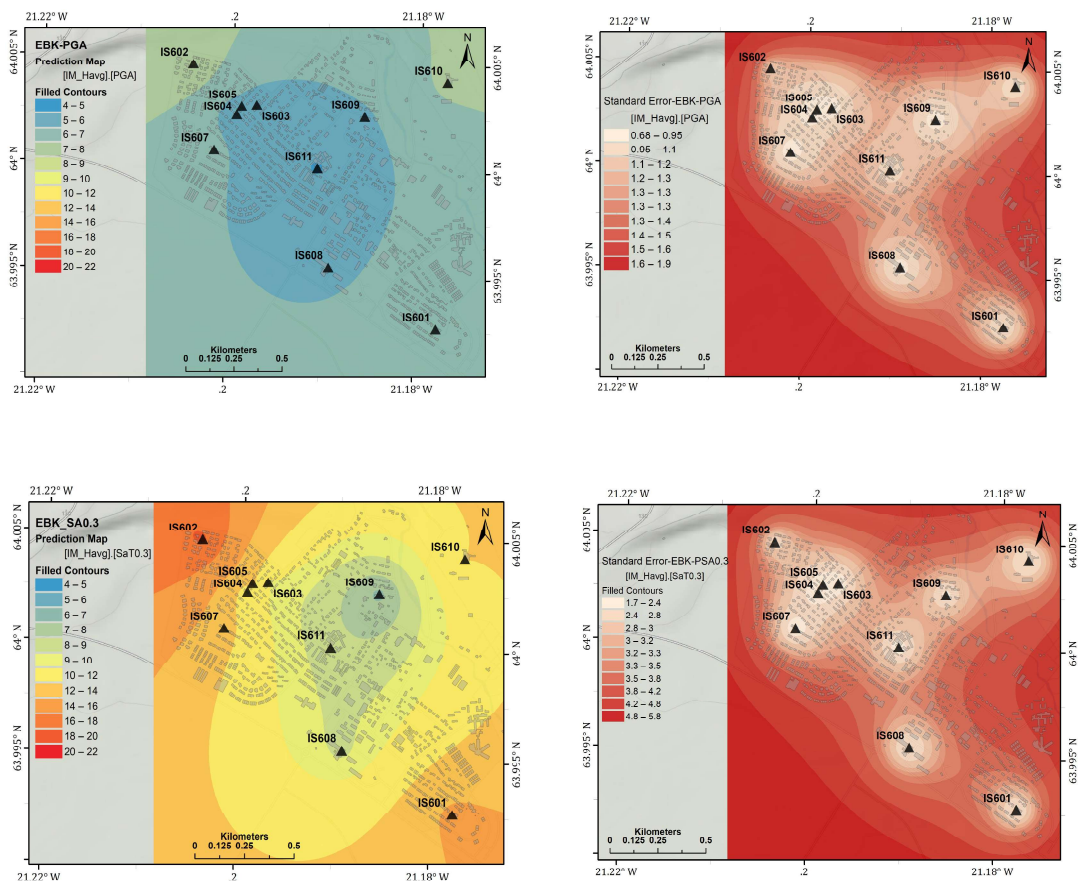


Fig. 3 - Shake maps of PGA ( $m/s^2$ ) and PSA at  $T=0.3$  sec (left panels) along with their standard error maps (right panels) across Hveragerði. Buildings are indicated by light grey polygons.

From the spatial distribution of IMs in Fig. 3, we observe a consistent spatial pattern with persistently lower IM levels in the central part of Hveragerði (see IS608, IS611, and IS609 sites) are located, while largest IMs being observed/estimated on the E-W outskirts of town. This pattern was consistently seen for peak parameters at short and intermediate natural periods but not at long periods. The clue as to why the central part of the town

exhibits lower motions may be found in the town's geology. A historical earthquake N-S fault has been mapped and lies directly through the center of town (west of IS609, under IS611 and IS608 stations, and further south). Furthermore, the fault serves as a conduit for geothermal water that reaches the surface, resulting in a geothermal area in the center of town and a widespread and elevated ground temperature gradient around IS611 and towards the north (Sæmundsson and Kristinsson 2005). Then, underneath the surficial lava layer of several meters is a softer sedimentary layer, resulting not only in a velocity reversal but has been affected by the geothermal activity (Rahpeyma et al. 2016). Therefore, this elongated area is believed to attenuate higher-frequency motions more effectively than the outskirts of town, where this effect is not observed in local geology, and not in the strong-motion data. These spatial differences in geology are also what is believed to contribute to the large scatter in the observed high-frequency motions. Eventually, we notice that at longer periods, the size of the small-aperture array becomes comparable in size or even small compared to the seismic wavelengths, and such small-spatial scale effects are less systematically observed (see Darzi et al. 2021, 2022).

The near-fault seismic ground motion recordings were characterized by intense accelerations of a relatively short duration of 5-6 seconds and large amplitude near-fault velocity pulses. The variation of horizontal PGA in the area is considerable given the small area of the array, having a minimum between 4.3 to 5.2  $\text{m/s}^2$  in the centre of Hveragerði to a maximum of a maximum of 7.3-8.7  $\text{m/s}^2$  in the eastern and western parts of the town. The shakemap of the short-period PSA shows that the mean values of PSAs at 0.3 sec exceed 10  $\text{m/s}^2$  ( $\sim 1.0$  g). It is interesting to note that the vast majority of the building stock that suffered the earthquake experienced much larger accelerations than the code design value specified, i.e., 20%g for buildings built before 2002 when no design spectrum was implicitly defined (Sigbjörnsson et al. 2009).

#### 4. Seismic Risk Assessment

The main objective of this study is to perform a seismic risk assessment for the  $M_w 6.3$  Ölfus earthquake scenario, evaluating different risk metrics: mean damage ratio (MDR) and damage probability at five damage states (DS), and for each building typology. Furthermore, we compare the performance of the most recent fragility curves developed based on local empirical damage data (Bessason et al. 2022) and applicable for events in 6.2-6.4  $M_w$  range with the global fragility curves (Martins and Silva 2020). To do this, the open-source algorithm, SELENA (Molina et al. 2010), is adapted to estimate the seismic loss at the building-by-building level across Hveragerði town.

Having complete building property database, the main building typologies are identified according to the SERA taxonomy system (Crowley et al. 2020) based on their level of ductility, material, LLRS, and height. Table 2 and 3 show the model building typologies for Hveragerði building stocks by building classes for which local, Bea22 (Bessason et al. 2022), and global fragility functions, MS20 (Martins and Silva 2020), were available. Considering the low-rise buildings in Hveragerði, the local and global fragility models attributed to either PGA or PSA at  $T=0.3$  sec are used dependent on building height and availability of the fragility model. To account for two sources of uncertainty, i.e., ground motion IM estimation and monetary loss values, a logic tree framework is employed with weighted branches associated with mean, mean – standard deviation (lower bound), and mean + standard deviation (upper bound), corresponding to each building typology.

Table 2: Building typologies in accordance with local fragility curves

| Typology      | CR+CIP -<br>CDN+CDL | CR+CIP -<br>CDM+CDH | W+WLI-<br>CDN+CDL | W+WLI-<br>CDM+CDH | MR+CBH+MOC-<br>CDN+CDL |
|---------------|---------------------|---------------------|-------------------|-------------------|------------------------|
| Label         | CNL                 | CMH                 | WNL               | WMH               | MNL                    |
| No. buildings | 176                 | 245                 | 126               | 162               | 48                     |

Table 3: Building typologies according to the global fragility functions

| Typology      | CR_LWAL<br>-DUL H1 | CR_LWAL<br>-DUL H2 | CR_LWAL<br>-DUM H1 | CR_LWAL<br>-DUM H2 | W_LFM-<br>DUM H1 | W_LFM-<br>DUM H2 | MUR-CB99<br>LWAL-DNO H1 | MUR-CB99<br>LWAL-DNO H2 |
|---------------|--------------------|--------------------|--------------------|--------------------|------------------|------------------|-------------------------|-------------------------|
| Label         | CL1                | CL2                | CM1                | CM2                | W1               | W2               | M1                      | M2                      |
| No. buildings | 127                | 30                 | 240                | 24                 | 268              | 20               | 34                      | 14                      |

Fig. 4 shows the MDR (ratio of repair cost to new construction cost) predictions corresponding to 8 and 5 building typologies (Tables 2 and 3) as per global and local fragility models, respectively. In Fig. 4a, the discrepancy between MDRs from high- and classical-resolution risk assessment is insignificant, except for CL2, W2, M1, and M2 typologies where municipality level MDRs are greatly larger. The MDR estimates obtained from global MS20 models are plotted for both the classical municipality level (grey bars) and high-resolution of building-by-building level (see Darzi et al. 2022 for detailed information). The risk analyses using the Bea22 model was performed at a municipality level that is commonly used in regional loss modelling. Both Bea22 and MS20 results indicate that the most vulnerable building typologies are masonry. For Bea22, the least vulnerable buildings are those made of timber (WMH) with CDM and CDH design period in force and for MS20, the least vulnerable buildings belong to one-storey buildings RC buildings with medium and low ductile (CM1 and CL1). The impact of IM variability on MDRs is more highlighted in MS20 model estimates than the Bea22 model.

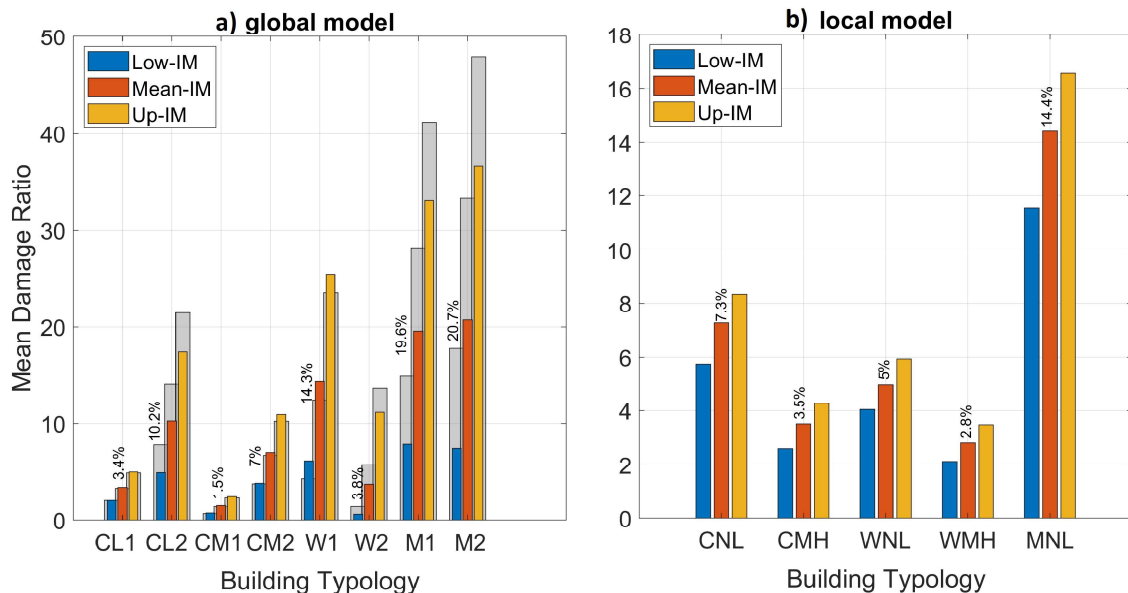


Fig. 4 - MDR estimates corresponding to a) eight and b) five building typologies associated with global in both high resolution and classical spatial resolution (grey bars) and local fragility models in classical resolution, respectively, for three IM levels. (see Darzi et al. 2022 for detailed information)

The damage probability corresponds to five damage states of complete collapse (DS4), extensive (DS3), moderate (DS2), slight (DS1), and no damage states (DS0). The DS4 to DS1 is determined by 100%, 60%, 20%, and 5% of the total normalized monetary values

according to the damage-to-loss model as recommended in global vulnerability model development (Martins and Silva 2020). Herein, the damage probability estimates are pooled for three main groups of concrete, timber, and masonry buildings in Iceland for a fair comparison between global and local fragility models.

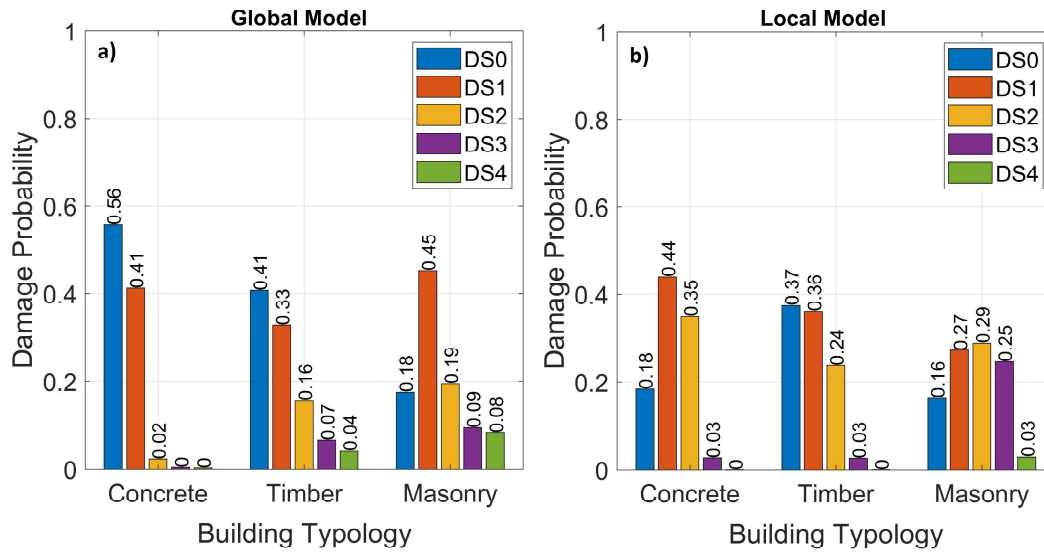


Fig. 5 – Damage probability predictions at 5 damage states for 3 material groups of buildings

The damage probability estimates corresponding to global (Fig. 5a) and local fragility models (Fig. 5b) at three material categories of buildings indicates larger number of buildings with no damage. For DS4, the local models' predictions are closer to actual observations as the actual observations of the in-situ survey conducted after the Ölfus earthquake showed that although the town suffered damages, there were minor extensive damages (DS3) and no collapses (DS4). Moreover, the non-structural components were the primary elements that were damaged.

## 5. Conclusions

In the seismic risk assessment, it is a common practice to perform risk analyses at a municipality geographical resolution (i.e., aggregate buildings within some predefined grid cell across the region of interest) and to assign only single IM to the grid. This study proved the necessity of conducting seismic risk assessment at high spatial resolution for reliable risk assessment, which is essential for emergency management planning and raising societal awareness of risk. The complete building exposure database gave us the unique opportunity to carry out detailed scenario-based loss assessment on a building-by-building level. More importantly, the dense spatial coverage of the ground motion records across Hveragerði available for  $M_w 6.3$ , May 29, 2008, Ölfus earthquake scenario allowed us to study the spatial variability of IMs at building coordinates employing the Empirical Bayesian Kriging geostatistical method and by that means to explore their impact on the expected loss measures. The significant variation of IMs over the small study area attributed to the non-uniform geology characterized by velocity reversals illustrates the significance of incorporating this source of variability. Such analyses result in a more reliable and informed view of the seismic risk at the study area.

Furthermore, we compared the risk predictions obtained from local and global fragility models over main building typologies identified across Hveragerði as per the SERA



classification scheme. Both local and global fragility models estimate that masonry buildings are the most vulnerable typology. It is of notice that masonry buildings are no longer constructed in Iceland which will help to mitigate the risk of future earthquakes. Overall, the local model showed better results in predicting the complete damaged buildings in Iceland than the global fragility curves. This emanates from the fact that the Icelandic buildings are constructed to withstand substantial lateral loads imposed by strong winds, which especially affects the design of lightweight structures like timber buildings. Additionally, for all building classes, the floor slabs and foundations are built highly earthquake-resistant using reinforced concrete that ties the foundations together. Additionally, generally, buildings are designed symmetrically in plan and height with well-designed wall LLRS. Thus, considering the unique structural and dynamic properties of buildings in Iceland as well as the large difference between risk metrics obtained from global and empirical local fragility models, we stress the necessity of analytical development of local fragility and vulnerability models that apply to the wide range of damaging earthquakes.

### Acknowledgements

The authors thank the Natural Catastrophe Insurance of Iceland for allowing access to their earthquake damage database. This study was funded by the Horizon 2020 TURNkey project [<https://earthquake-turnkey.eu/>] under grant agreement No 821046. It was also partly supported by a Postdoctoral grant (# 218255-051) from the Icelandic Research Fund.

### References

- Bessason B, Bjarnason JÖ, Rupakhety R (2020) Statistical modelling of seismic vulnerability of RC, timber and masonry buildings from complete empirical loss data. *Engineering Structures* 209:109969. <https://doi.org/10.1016/j.engstruct.2019.109969>
- Bessason B, Rupakhety R, Bjarnason JÖ (2022) Comparison and modelling of building losses in South Iceland caused by different size earthquakes. *Journal of Building Engineering* 46:103806. <https://doi.org/10.1016/j.jobee.2021.103806>
- Bjarnason JÖ, Einarsson P, Bessason B (2016) Iceland Catastrophe Insurance and Earthquake Risk Assessment. In: *International Workshop on Earthquakes in North Iceland*. Húsavík, North Iceland
- Costanzo A (2018) Shaking Maps Based on Cumulative Absolute Velocity and Arias Intensity: The Cases of the Two Strongest Earthquakes of the 2016–2017 Central Italy Seismic Sequence. *IJGI* 7:244. <https://doi.org/10.3390/ijgi7070244>
- Crowley H, Despotaki V, Rodrigues D, et al (2020) Exposure model for European seismic risk assessment. *Earthquake Spectra* 36:252–273. <https://doi.org/10.1177/8755293020919429>
- Crowley H, Despotaki V, Silva V, et al (2021) Model of seismic design lateral force levels for the existing reinforced concrete European building stock. *Bull Earthquake Eng* 19:2839–2865. <https://doi.org/10.1007/s10518-021-01083-3>
- Darzi A, Bessason B, Halldórsson B (2021) Ground Motion Intensity Measures, Variability and Seismic Loss Metrics, A Case Study for Hveragerði, South Iceland. In: *The 17th World Conference on Earthquake Engineering (17WCEE)*. Japan Association for Earthquake Engineering, Sendai, Japan,
- Darzi A, Bessason B, Halldórsson B, Molina, S., Kharazian, A., and Moosapoor, M. (2022) High spatial-resolution loss estimation using dense array strong-motion near-fault records. Case study for Hveragerði and the 6.3 Ölfus earthquake, South Iceland. *International Journal of Disaster Risk Reduction* (Accepted)

- Jónasson K, Bessason B, Helgadóttir Á, et al (2021) A Harmonised Instrumental Earthquake Catalogue for Iceland and the Northern Mid-Atlantic Ridge. *Natural Hazards and Earth System Sciences Discussions* 1–26
- Krivoruchko K, Gribov A (2019) Evaluation of empirical Bayesian kriging. *Spatial Statistics* 32:100368. <https://doi.org/10.1016/j.spasta.2019.100368>
- Martins L, Silva V (2020) Development of a fragility and vulnerability model for global seismic risk analyses. *Bull Earthquake Eng.* <https://doi.org/10.1007/s10518-020-00885-1>
- Molina S, Lang DH, Lindholm CD (2010) SELENA - An open-source tool for seismic risk and loss assessment using a logic tree computation procedure. *Computers and Geosciences* 36:257–269. <https://doi.org/10.1016/j.cageo.2009.07.006>
- Rahpeyma S, Halldorsson B, Olivera C, et al (2016) Detailed site effect estimation in the presence of strong velocity reversals within a small-aperture strong-motion array in Iceland. *Soil Dynamics and Earthquake Engineering* 89:136–151. <https://doi.org/10.1016/j.soildyn.2016.07.001>
- Rupakhety R, Sigbjörnsson R (2013) Rotation-invariant measures of earthquake response spectra. *Bulletin of Earthquake Engineering* 11:1885–1893
- Rupakhety R, Sigbjörnsson R, Ólafsson S (2016) Damage to residential buildings in Hveragerði during the 2008 Ölfus Earthquake: simulated and surveyed results. *Bull Earthquake Eng* 14:1945–1955. <https://doi.org/10.1007/s10518-015-9783-5>
- Sæmundsson K, Kristinsson S (2005) Hveragerði. Hitamælingar í jarðvegi og sprungur (Hveragerði: Soil temperature measurements and faults). Iceland GeoSurvey (ÍSOR), Reykjavík, Iceland
- Sigbjörnsson R, Ólafsson S, Snæbjörnsson JTh (2007) Macroseismic effects related to strong ground motion: a study of the South Iceland earthquakes in June 2000. *Bull Earthquake Eng* 5:591–608. <https://doi.org/10.1007/s10518-007-9045-2>
- Sigbjörnsson R, Snæbjörnsson JT, Higgins SM, et al (2009) A note on the M w 6.3 earthquake in Iceland on 29 May 2008 at 15:45 UTC. *Bulletin of Earthquake Engineering.* <https://doi.org/10.1007/s10518-008-9087-0>
- Standards Council of Iceland / Staðlaráð Íslands (SI) (2010) Icelandic National Annexes to EUROCODES. Staðlaráð Íslands, Reykjavík, Iceland
- Standards Council of Iceland/ Staðlaráð Íslands (SI) (2002) National Application Documents (NAD) for Iceland
- Tryggvason E, Thoroddsen S, Thorarinsson S (1958) Report on earthquake risk in Iceland. *Timarit Verkfraedingafelags Íslands* 43:81–97
- (1976) ÍST 13, Earthquakes, Loads and Design Rules. Icelandic Industrial Development Agency / Idnþróunarstofun Íslands, Reykjavík, Iceland
- (1989) ÍST 13, Earthquakes, Loads and Design Rules. Icelandic Industrial Development Agency / Idnþróunarstofun Íslands, Reykjavík, Iceland